

Changes induced by the *Pepper mild mottle tobamovirus* on the chloroplast proteome of *Nicotiana benthamiana*

M. Pineda · C. Sajnani · M. Barón

Received: 19 December 2008 / Accepted: 21 September 2009 / Published online: 10 October 2009
© Springer Science+Business Media B.V. 2009

Abstract We have analyzed the chloroplast proteome of *Nicotiana benthamiana* using two-dimensional gel electrophoresis and mass spectrometry followed by a database search. In order to improve the resolution of the two-dimensional electrophoresis gels, we have made separate maps for the low and the high pH range. At least 200 spots were detected. We identified 72 polypeptides, some being isoforms of different multiprotein families. In addition, changes in this chloroplast proteome induced by the infection with the Spanish strain of the *Pepper mild mottle virus* were investigated. Viral infection induced the down-regulation of several chloroplastidic proteins involved in both the photosynthetic electron-transport chain and the Benson–Calvin cycle.

Keywords Biotic stress · Chloroplast proteome · Multiprotein families · *Nicotiana benthamiana* · *Pepper mild mottle virus* · Two-dimensional gel electrophoresis

Abbreviations

2-DE Two-dimensional gel electrophoresis

Pineda, M and Sajnani, C, These authors have contributed equally to this work and are placed in alphabetical order.

M. Pineda · C. Sajnani · M. Barón (✉)
Department of Biochemistry, Molecular and Cellular Biology of Plants, Estación Experimental del Zaidín, (CSIC) C/Profesor Albareda no. 1, C.P. 18008 Granada, Spain
e-mail: mbaron@eez.csic.es

CF ₁	ATP-ase coupling factor
CP	Coat protein
Cyt. f	Cytochrome f
FNR	Ferredoxin-NADP ⁺ reductase
GS	Glutamine synthetase
Hsp70	Heat-shock protein 70 kDa
IEF	Isoelectrofocusing
Lhca	Photosystem I chlorophyll a/b binding proteins
Lhcb	Photosystem II chlorophyll a/b binding proteins
MALDI	Matrix-assisted laser desorption/ionization
M _r	Relative molecular mass
MS	Mass spectrometry
OEC	Oxygen-evolving complex
PGK	Phosphoglycerate kinase
pI	Isoelectrical point
PMMoV-S	Spanish strain of <i>Pepper mild mottle virus</i>
PRK	Phosphoribulokinase
PsaC, PsaD and PsaE	C, D and E proteins, respectively of the photosystem I core complex
PsbO, PsbP and PsbQ	33, 24 and 16 kDa extrinsic proteins of the photosystem II oxygen-evolving complex
PSI	Photosystem I
PSII	Photosystem II
RbcL and RbcS	Ribulose 1,5 bisphosphate carboxylase oxygenase large and small subunits, respectively
RuBisCO	Ribulose 1,5 bisphosphate carboxylase oxygenase
Rca	Ribulose 1,5 bisphosphate carboxylase oxygenase activase

SBPase
TOF/TOF
Sedoheptulose-1,7-bisphosphatase
Time-of-flight tandem mass spectrometry

Introduction

Proteomics is, at present, an irreplaceable tool to study the response of living organisms to their environment. However, less attention has been applied to the plant proteome, although some reviews on this topic have been published in recent years (Rossignol 2001; Bagginsky and Gruissem 2004; Cánovas et al. 2004; Newton et al. 2004; Rose et al. 2004; van Wijk 2004; Rossignol et al. 2006; Jorrín et al. 2007, 2009). In order to improve the understanding of plant proteome expression, a number of studies have focused on organelle subproteomes, such as those of chloroplast and mitochondria responsible for the plant energy metabolism. Two-dimensional gel electrophoresis (2-DE), consisting of isoelectrofocusing (IEF) followed by SDS-PAGE electrophoresis (IEF/SDS-PAGE), was one of the first techniques applied to study the chloroplast proteome. This approach has proven successful for the analysis of both luminal and peripheral thylakoid proteins from *Pisum sativum* (Peltier et al. 2000) and *Arabidopsis* (Kieselbach et al. 2000; Peltier et al. 2002; Schubert et al. 2002). Blue-native polyacrylamide gel electrophoresis followed by SDS-PAGE (2-DE BN/SDS-PAGE), commonly used to characterize chloroplast protein complexes in plants and algae (Schägger et al. 1994), has also provided an excellent two-dimensional alternative for the IEF/SDS-PAGE in the case of the most hydrophobic thylakoid proteins. This technique has provided insight into the chloroplast proteome of *Hordeum vulgare* (Ciambella et al. 2005) and *Cucurbita pepo* (Aro et al. 2005). Several strategies (fractionation followed by multi-dimensional protein-separation steps) have also been used to identify the hydrophobic thylakoid integral membrane proteome (Friso et al. 2004; Peltier et al. 2004), as well as to decipher the chloroplast envelope proteome (Ferro et al. 2002) of *Arabidopsis*. In addition, novel non-gel proteomic techniques have revealed the pathway abundance and novel protein functions in the photosynthetic membranes (Huber et al. 2004; Kleffman et al. 2004).

Fewer efforts have been made to identify the changes on the proteomic profile of chloroplast from plants undergoing different biotic and abiotic-stress factors. Phee et al. (2004) and Giacomelli et al. (2006) analyzed the response of the chloroplast proteome to high light in *Arabidopsis thaliana*; Andaluz et al. (2006) and Laganowsky et al. (2009) studied the proteomic changes induced by iron deficiency in the

thylakoid membranes from *Beta vulgaris* and *A. thaliana*, respectively; Cui et al. (2005) investigated the chloroplast proteome as the main target of cold stress in *Oryza sativa*. Recently, Taylor et al. (2009) reviewed the changes induced by abiotic stress in the proteome of some organelles, including the chloroplast. Using 2-DE, Jones et al. (2006) detected significant changes in the chloroplast proteome of *Arabidopsis* plants infected with *Pseudomonas syringae* pv. *tomato*; photosystem II (PSII) and the Benson–Calvin cycle were revealed as the most affected processes. Zhou et al. (2006) carried out a proteomic analysis of the compatible interaction *Fusarium graminearum* and *Triticum aestivum* and concluded that the chloroplast is the organelle mostly affected by the infection. A leaf proteomic approach was also carried out to study pea responses to powdery mildew, and showed changes in proteins involved in photosynthesis and carbon metabolism in the host plant (Curto et al. 2006).

By using 2-DE, we have previously investigated the changes in the protein pattern of the oxygen-evolving complex (OEC) of PSII during the infection of *Nicotiana benthamiana* plants with the Spanish strain of the *Pepper mild mottle tobamovirus* (PMMoV-S) (Pérez-Bueno et al. 2004). We demonstrated that the OEC is one of the main targets of the viral infection in the chloroplast (Rahoutei et al. 2000). The proteomic analysis of the OEC from the infected plants showed that the PsbO and PsbP proteins correspond to protein families in *N. benthamiana*, and the content of the PsbP polypeptides decreased dramatically with respect to PsbO during the infection progress. Notably, there was a differential decrease of the various PsbP proteins, indicative of a different regulation of their expression during pathogenesis (Pérez-Bueno et al. 2004).

In the present study, we delve further into the analysis of the chloroplast proteome of *N. benthamiana* by using 2-DE and mass spectrometry (MS) followed by database searching. *Nicotiana benthamiana* is one of the most common experimental hosts and it is used in many studies on compatible plant–virus interactions, because of its susceptibility to infection by many different viral families. Progress in the knowledge of the *N. benthamiana* chloroplast proteome would be of high interest in the field of the impact of biotic stress on photosynthesis. In addition, PMMoV-S-induced changes in the chloroplast proteome after 14 days post-inoculation (dpi) were investigated. Our previous studies showed that this time span was one of the most representative of the PMMoV-S infections (Rahoutei et al. 2000; Pérez-Bueno 2003; Chaerle et al. 2006; Sajani et al. 2007). The present proteomic study revealed that viral infection induced the down-regulation of several photosynthetic proteins involved in both the photosynthetic electron-transport chain and the Benson–Calvin cycle.

Materials and methods

Plant and virus material

Nicotiana benthamiana Gray plants were cultivated in a growth chamber at $100 \mu\text{mol m}^{-2} \text{s}^{-1}$ photosynthetically active radiation, provided by cool white fluorescent lamps, with a 16/8 h light/dark photoperiod, a temperature regime of 23/18°C (day/night), and a relative humidity of 65%. Plants at the stage of 6–7 fully expanded leaves were inoculated in the three lower leaves with 25 μl of inocula (50 $\mu\text{g/ml}$ of purified PMMoV-S solution in 20 mM sodium phosphate buffer pH 7.0) per leaf. Mock-inoculated plants were treated only with buffer. The Spanish strain of PMMoV (genus Tobamovirus) was isolated in Almería, Spain (Alonso et al. 1989).

Visual symptoms and sample isolation

Plants infected with PMMoV-S developed new curly leaves at 5–6 dpi. Growth was inhibited in infected plants compared with the controls at 14 dpi. At 22–24 dpi, infected plants were totally senescent. For a more detailed description of symptoms, see Pineda et al. (2008b).

Chloroplast-enriched preparations from virus-infected plants and their corresponding controls were isolated according to Reche et al. (1997) at 14 dpi. For this purpose, we selected 8 g of plant material (curly and non-curly leaves from infected plants, as well as their homologous controls). Then, leaves were homogenized 4 s at 9.3 g (Polytron, Kinematica; Lucerne, Switzerland) in 35 ml of semi-frozen homogenization buffer [0.33 M sorbitol, 50 mM 4-(2-hydroxyethyl)-1-piperazineethanesulfonic acid (HEPES)-KOH pH 7.5, 0.1% serum bovine albumin, 2 mM ethylenediaminetetraacetic acid (EDTA), and 1 mM Cl_2Mg]. Next, the homogenate was filtered through four layers of miracloth and placed in Sorvall tubes. A layer of Percoll (40% in homogenization buffer) was deposited in the bottom of the tube (14 ml Percoll solution per 17 ml homogenate) and then centrifuged at 7,000g for 1 min at maximum speed and at 4°C (Sorvall RC5C centrifuge, SS-34 rotor; Thermo Fisher Scientific Inc., Waltham, USA). The supernant was removed and 400 μl of lysis buffer (5 mM Cl_2Mg) were added to the chloroplast pellet before centrifuging at 13,000g for 10 min at 4°C. The pellet, containing the chloroplast-enriched preparations, was resuspended in 200 μl of sample buffer (0.33 M sorbitol, 50 mM Hepes-KOH pH 7.5). Aliquots were stored at -70°C .

Sample solubilization for protein electrophoresis

Sample solubilization was carried out according to Schuster and Davies (1983) with minor modifications.

First, 200 μl from a chloroplast-enriched preparation containing 1 μg Chl/ μl was incubated with 200 μl extraction buffer [0.7 M sucrose, 0.5 M Tris, 30 mM HCl, 50 mM EDTA, 0.1 M KCl, 2% (v/v) 2-mercaptoethanol, and 2 mM phenylmethylsulphonyl fluoride (PMSF)] for 20 min at 4°C, vortexing several times. Then, 400 μl of 0.1 M Tris-HCl-saturated phenol (Amresco, Ohio, USA) were added. After 15 min of shaking at 4°C, the phases were separated by 10 min centrifugation at 16,000g and 4°C. The phenolic phase was recovered and re-extracted three times with an equal volume of extraction buffer, as mentioned above. Proteins were precipitated from the phenol phase by adding 6 volumes of 0.1 M ammonium acetate in methanol (HPLC grade) and incubated at -20°C overnight. The pellet, after a centrifugation for 10 min at 16,000g and 4°C, was washed three times with the ammonium acetate-methanol solution and then 8 volumes of 100% HPLC acetone was added. Proteins were kept at -20°C at least for 4 h and then precipitated under the same centrifugation conditions. The pellet was dried and solubilized in ReadyPrep Sequential Extraction Reagent 3 (BioRad; Hercules, CA, USA), containing 5 M urea, 2 M thiourea, 2% (w/v) CHAPS, 2% (w/v) SB 3–10, 40 mM Tris, 0.2% Bio-Lyte 3/10, and 2 mM TBP. The sample was incubated for 2 h at room temperature under gentle shaking. Insoluble material was removed by centrifugation for 10 min at 16,000g and 25°C. The protein content of the sample was measured using the 2-D Quant Kit (GE Health Care; St. Giles Chalfont, United Kingdom). After quantification, pI (isoelectrical point) standards (2-D SDS-PAGE Standards, BioRad) were added to samples used for alkaline (6–11) pH range gels.

First-dimension electrophoresis: isoelectrofocusing (IEF)

IEF was carried out on 11 cm ReadyStrip IPG Strip gels (BioRad) as well as on Immobiline DryStrip gels (GE Health Care) for the 4–7 and 6–11 pH ranges, respectively. The strips were allowed to rehydrate in a PROTEAN IEF Cell (BioRad) for 14–16 h at 50 V and 20°C with 200 μl of chloroplast preparation, containing 75 μg of proteins and a trace of bromophenol blue. Proteins were separated in the pH range 4–7 by IEF using a three-step procedure: 15 min at 250 V, followed by 2 h at 8,000 V and a final step of 8,000 Vh to complete 35,000 Vh. In the case of the 6–11 pH range, some intermediate steps were required according to Görg et al. (2000): 1 h at 150 V, 1 h at 300 V, 1 h at 1,000 V, 1 h at 3,000 V, 1 h at 6,000 V, and 6,000 Vh to complete 25,000 Vh. After focusing, the strips were immediately run or frozen at -80°C .

SDS-PAGE

Focused IEF strips were incubated at room temperature for 20 min with two changes of equilibration buffer, 50 mM Tris-HCl, pH 8.8, containing 6 M urea, 2% (w/v) SDS, 0.02% (w/v) bromophenol blue, 30% glycerol, and 0.5% (w/v) DTT (dithiothreitol). Strips were then layered on the top of a SDS 12% polyacrylamide gel and sealed with melted 0.8% agarose in running buffer. Then two gels were run simultaneously, one per treatment, in order to reduce variability. Running conditions were 17 mA for 30 min and 48 mA for 5–6 h. After electrophoresis, the gels were silver-stained (pH 6–11 map; Yan et al. 2000) or Sypro Ruby-stained (pH 4–7 map; BioRad, Steinberg et al. 1996). In order to ensure the reproducibility of the results, triplicate 2-DE gels were made from three independent chloroplast preparations, each from a different batch of plants. Gels were scanned and analysed using the ImageJ software (<http://rsb.info.nih.gov/ij>). The intensity of every spot of interest, as well as its corresponding area, were measured and then compared between gels from control and infected plants, according to the following equation:

Difference

$$= \left[1 - \left(\frac{\text{area}_{\text{PMMoV-S}} \cdot \text{intensity}_{\text{PMMoV-S}}}{\text{area}_{\text{control}} \cdot \text{intensity}_{\text{control}}} \right) \right] \cdot 100$$

Only differences higher than 30% were considered as significant. Figures show the most representative gels.

Mass spectrometry and protein identification

Spots from silver- or Sypro Ruby-stained gels were manually excised and stored in milli-Q water at 4°C until MALDI-TOF/TOF (matrix-assisted laser desorption/ionization coupled to time-of-flight tandem mass spectrometry) analysis. Protein spots were digested automatically using a Proteineer DP protein digestion station (Bruker-Daltonics; Bremen, Germany). The digestion protocol used was that of Schevchenko et al. (1996) with minor variations. For peptide mass fingerprinting and TOF/TOF spectra acquisition an aliquot of *a*-cyano-4-hydroxycinnamic acid in 33% aqueous acetonitrile and 0.1% trifluoroacetic acid was mixed with an aliquot of the above digestion solution and the mixture was deposited onto an AnchorChip MALDI probe (Bruker-Daltonics). Peptide mass fingerprint spectra were measured on a Bruker Ultraflex MALDI-TOF/TOF mass spectrometer (Bruker-Daltonics) (Suckau et al. 2003) in positive ion reflector mode. When possible, mass measurements were performed automatically through fuzzy-logic-based software. Each spectrum was internally calibrated with mass signals of trypsin autolysis ions to reach a typical mass-measurement accuracy of ± 25 ppm. The measured tryptic

peptide masses were transferred through MS BioTools program (Bruker-Daltonics) as inputs to search the NCBI Inr database using Mascot software (Matrix Science; London, UK). MS/MS data from LIFT-TOF/TOF spectra were combined with MS peptide mass fingerprint data for database searching. Positively identified proteins are listed in Tables 1 and 2.

Results

Chloroplastidic proteins from both control and PMMoV-S infected *N. benthamiana* plants were separated by 2-DE and the resulting gels were analyzed in order to detect the changes induced by the viral infection. In order to improve the gel resolution, separate 2-DE maps were made for the low (4–7) and high (6–11) pH ranges.

Chloroplast proteome of control *Nicotiana benthamiana* plants in the pH range 4–7

Most of the chloroplastidic proteins were found in this pH range. At least 150 spots could be detected in the 2-DE gel (Fig. 1a, b). Based on the reproducibility of the spot pattern and relative amount of the proteins, 78 spots were selected for the MALDI-TOF/TOF analysis. A number of 55 proteins could be identified (Table 1, spots # 1–55). Most of the proteins identified (31) were members of the different photosynthetic complexes of the thylakoid membrane: 16 polypeptides from PSII, three proteins from photosystem I (PSI), two cytochrome *f* (Cyt. *f*) polypeptides from the cytochrome complex and 10 spots corresponding to the ATP synthase. PSII proteins belonging to the OEC were one of the most abundant proteins in the gels. Six spots corresponding to the PsbO multiprotein family were found (# 1–6), showing the same M_r (relative molecular mass) and different pI (isoelectrical point). The PsbP multiprotein family contributed with 10 spots (# 7–16), six of them (# 7–11, 16) with similar M_r and differing in pI as well as four spots (# 12–15) of lower M_r . From PSI, we detected the ferredoxin-NADP⁺-reductase (# 19), PsaC (# 31), and a *cab* protein from the light-harvesting complex of PSI (Lhca; # 32). In addition, we identified 2 Cyt. *f* polypeptides (# 18 and 20) from the cytochrome complex. The ATP synthase macrocomplex was represented by 10 proteins (# 21–30), corresponding to the five subunits of the CF₁ catalytic portion: α (# 25–27), β (# 22–24), γ (# 21), δ (# 28), and ϵ (# 29 and 30). Spots corresponding to the same subunit showed the same M_r but different pI.

Concerning the proteins involved in the Benson–Calvin cycle, the RuBisCO (ribulose 1,5 bisphosphate carboxylase oxygenase) was the most prominent protein in the 2-DE gel. RbcL (RuBisCO large subunit, # 36) was present in the

Table 1 Proteins identified by MALDI/TOF-TOF from the 2-DE showed in Figs. 1 and 2 and marked by the same number

Spot	Homology	Species	Accession #	Theoretical mass	Theoretical pI	Experimental mass	Experimental pI	Mascot score	Matched peptides	Unmatched peptides	% Coverage
1	PsbO	*	gi 30013657	35	5.3	35.4	5.1	152	10	3	26
2	PsbO	*	gi 30013657	35	5.3	35.4	5.2	85	5	1	20
3	PsbO	*	gi 30013657	35	5.3	35.4	5.3	124	7	1	27
4	PsbO	*	gi 30013657	35	5.3	35.4	5.5	96	6	3	33
5	PsbO	*	gi 30013657	35	5.3	35.4	5.7	182	11	2	42
6	PsbO	*	gi 30013657	35	5.3	35.4	5.8	189	10	0	37
7	PsbP	*	gi 19911	29	7.5	26.2	5.1	125	6	1	33
8	PsbP	*	gi 19911	29	7.5	26.2	5.3	108	7	6	39
9	PsbP	*	gi 49259455	19	5.1	26.2	5.5	105	5	2	37
10	PsbP	*	gi 49259455	19	5.1	26.2	5.8	105	5	2	37
11	PsbP	*	gi 49259455	19	5.1	26.2	6.1	106	5	2	37
12	PsbP	*	gi 1345550	29	7.5	23.2	5.3	96	5	1	26
13	PsbP	*	gi 1345550	29	7.5	23.2	5.5	121	6	1	29
14	PsbP	*	gi 1345550	29	7.5	23.2	5.8	113	6	2	33
15	PsbP	*	gi 1345550	29	7.5	23.2	6.1	80	4	1	25
16	PsbP	*	gi 49259455	19	5.1	26.2	6.4	82	4	2	37
17	Plastid lipid associated protein	*	gi 2632088	29	4.6	37.9	5.0	122	7	4	25
18	Cyt. f	*	gi 65614	35	8.2	37.9	6.5	163	9	–	42
19	FNR, chain b	<i>Capsicum annuum</i>	gi 47169164	34	–	37.9	6.3	171	7	16	–
20	Cyt. f	*	gi 1465970	35	8.2	37.9	6.1	92	6	4	18
21	CF1 γ	*	gi 19785	42	7.6	43.8	6.6	109	7	2	17
22	CF1 β	<i>Nicotiana plumbaginifolia</i>	gi 14556	54	4.9	59.0	5.7	196	13	7	37
23	CF1 β	<i>Nicotiana plumbaginifolia</i>	gi 14556	54	4.9	59.0	5.9	230	16	10	42
24	CF1 β	<i>Naphar variegata</i>	gi 4718153	51	4.7	59.0	6.1	108	6	0	16
25	CF1 α	*	gi 5597763	55	4.9	59.0	5.5	240	15	2	31
26	CF1 α	*	gi 5597763	55	4.9	59.0	5.7	269	16	1	35
27	CF1 α	<i>Atropa belladonna</i>	gi 28261702	55	5	59.0	5.9	183	11	1	23
28	CF1 δ	*	gi 19787	27	8.1	20.1	5.3	85	6	5	24
29	CF1 ϵ	<i>Atropa belladonna</i>	gi 28261723	15	5	16.1	5.4	114	5	1	43
30	CF1 ϵ	*	gi 1465963	15	5	16.2	5.7	117	6	4	51
31	Putative PsC	<i>Solanum tuberosum</i>	gi 34787119	9	6.9	11.1	6.3	145	6	1	71
32	Lhca Type III	<i>Lycopersicon esculentum</i>	gi 19182	29	–	30.1	6.4	67	–	–	–
33	Thylakoid lumenal 16.5 kDa protein	<i>Arabidopsis thaliana</i>	gi 7388292	26	–	14.8	5.0	80	–	–	–

Table 1 continued

Spot	Homology	Species	Accession #	Theoretical mass	Theoretical pI	Theoretical mass	Experimental mass	Experimental pI	Mascot score	Matched peptides	Unmatched peptides	% Coverage
34	RbcS	<i>Flaveria ramosissima</i>	gi13241101	16	–	–	12.9	5.7	98	4	8	–
35	RbcS	<i>Chrysanthemum x morifolium</i>	gi28139169	21	–	–	12.9	6.0	116	5	7	–
36	RbcL	<i>Nolana albescens</i>	gi11182397	52	6.5	–	58.5	6.9	87	6	3	16
37	Hypothetical protein	<i>Arabidopsis thaliana</i>	gi7267602	49	–	–	57.7	4.7	62	–	–	–
38	60 kDa chaperonin α subunit, RuBisCo-binding protein	<i>Brassica napus</i>	gi1351030	58	4.6	–	66.7	5.2	123	7	0	18
39	FtsH like	*	gi4325041	75	6	–	69.3	5.6	101	6	0	12
40	Hsp70	<i>Pisum sativum</i>	gi445605	76	–	–	73.1	5.1	108	5	1	–
41	Hsp70	<i>Pisum sativum</i>	gi445605	76	–	–	72.5	5.1	106	4	0	–
42	GS	<i>Nicotiana attenuata</i>	gi40457328	48	6.8	–	49.9	5.9	94	6	3	16
43	GS	<i>Nicotiana attenuata</i>	gi40457328	48	6.8	–	49.9	6.0	92	6	2	12
44	GS	<i>Nicotiana attenuata</i>	gi40457328	48	6.8	–	49.9	6.1	125	8	3	22
45	SBPase	<i>Spinacia oleracea</i>	gi3914940	43	–	–	47.3	5.3	80	–	–	–
46	PRK	<i>Spinacia oleracea</i>	gi21279	45	5.8	–	45.5	5.5	89	6	4	15
47	Rea	*	gi19990	49	7.6	–	48.7	5.6	176	13	9	29
48	Rea	*	gi19990	49	7.6	–	48.7	5.7	119	10	12	25
49	PGK	*	gi1161600	50	8.5	–	48.7	5.8	206	8	–	20
50	Rea	*	gi445628	43	5.5	–	48.7	5.8	–	8	7	22
51	PGK	*	gi1161600	50	8.5	–	48.7	5.9	205	8	–	–
52	SFBA	<i>Nicotiana paniculata</i>	gi4827251	43	7	–	41.2	6.0	104	7	4	21
53	SFBA	<i>Nicotiana paniculata</i>	gi4827251	43	7	–	41.2	5.8	94	6	3	16
54	SFBA	<i>Nicotiana paniculata</i>	gi4827251	43	7	–	41.2	6.1	90	6	4	16
55	CP	<i>ToMV (tobamovirus)</i>	gi10719965	17	–	–	17.6	6.2	99	5	2	15
56	Cyt. f	*	gi11845	35	8.2	–	40.2	5.2	159	9	7	–
57	PsaD	<i>Nicotiana sylvestris</i>	gi19748	22	8.8	–	17.9	7.0	145	8	1	23
58	PsaD	<i>Nicotiana sylvestris</i>	gi19748	22	8.8	–	17.9	8.7	106	6	2	32
59	PsaD	<i>Nicotiana sylvestris</i>	gi19748	22	8.8	–	17.9	9.0	112	6	1	31
60	PsaD	<i>Nicotiana sylvestris</i>	gi19748	22	8.8	–	17.9	9.2	113	6	1	28
61	PsaD	<i>Nicotiana sylvestris</i>	gi417544	23	8.8	–	16.7	9.3	129	7	3	44
62	PsaD	<i>Nicotiana sylvestris</i>	gi19748	22	8.8	–	16.7	9.3	105	6	4	26
63	PsaD	<i>Nicotiana sylvestris</i>	gi19748	22	8.8	–	16.7	9.2	133	7	2	43
64	PsaD	<i>Nicotiana sylvestris</i>	gi19748	22	8.8	–	16.7	9.0	107	–	–	–
			gi19748	22	8.8	–	16.7	8.7	85	–	–	–

Table 1 continued

Spot	Homology	Species	Accession #	Theoretical mass	Theoretical pI	Experimental mass	Experimental pI	Mascot score	Matched peptides	Unmatched peptides	% Coverage
65	PsbQ	<i>Nicotiana benthamiana</i>	gi58700507	24	8.7	10.9	9.4	163	8	0	32
66	PsbQ	<i>Nicotiana benthamiana</i>	gi58700507	24	8.7	10.9	9.5	123	6	0	24
67	PsaE	<i>Nicotiana sylvestris</i>	gi632722	15	8.6	13.9	8.2	133	7	6	43
68	PsaE	<i>Nicotiana sylvestris</i>	gi632724	15	8.7	13.9	8.8	130	7	7	54
69	Ribosomal protein L14	<i>Nicotiana sylvestris</i>	gi178102574	14	–	7.3	9.2	220	6	0	–
70	CF1 α	*	gi176559637	55	4.9	77.3	6.4	117	7	1	18
71	Lhcb	<i>Nicotiana sylvestris</i>	gi3036944	28	–	34.8	6.7	96	4	6	–

Each polypeptide is annotated with the homology found, including protein name, plant species and the corresponding protein accession number. * indicate *Nicotiana tabacum*. Theoretical and experimental pIs and M_r are also provided. Homologies include the % coverage reached, the number of matched and unmatched peptides, and the Mascot score details. Scores > 76 are significant ($P < 0.05$)

CF₁ ATP synthase catalytic portion; CP viral-coat protein; Cyt. f cytochrome f; FNR ferredoxin-NADP⁺ reductase; GS glutamine synthetase; Hsp70 heat shock protein 70 kDa; Lhca PSI chlorophyll a/b binding proteins; Lhcb PSII chlorophyll a/b binding proteins; PGK phosphoglycerate kinase; PRK phosphoribulo-kinase; Psa proteins PSI proteins codified by *psa* genes; Psb proteins PSII proteins codified by *psb* genes; RbcL RuBisCO large subunit; RbcS RuBisCO small subunit; Rca RuBisCO activase; SBPase sedoheptulose-1,7-bisphosphatase; SPBA sedoheptulose/fructose-bisphosphate aldolase

Table 2 pI standards identified by MALDI/TOF-TOF from gels displayed in Fig. 2

Spot	Homology	Species	Accession #	Theoretical mass	Theoretical pI	Experimental mass	Experimental pI	Mascot score	Matched peptides	Unmatched peptides	% Coverage
a	Glyceraldehyde-3-phosphate dehydrogenase	–	gi2506441	36	7.9	47.6	7.5	105	6	1	16
b	Glyceraldehyde-3-phosphate dehydrogenase	–	gi1169794	36	7.9	46.0	8	126	7	1	20
c	Glyceraldehyde-3-phosphate dehydrogenase	–	gi40889053	36	7.8	46.0	8.4	188	10	1	28
d	Glyceraldehyde-3-phosphate dehydrogenase	–	gi1169794	36	7.9	46.0	8.6	107	6	1	16
e	Bovine carbonic anhydrase II, chain B	–	gi46016009	29	6.5	35.0	6.4	202	10	1	33
f	Horse Herat myoglobin	<i>Equus caballus</i>	gi2554649	17	7.5	10.9	7.8	185	9	2	63
g	Albumin	<i>Bos taurus</i>	gi1162648	71	5.8	10.0	8.9	145	11	4	21

Each polypeptide is annotated with the homology found, including protein name, species and the corresponding protein accession number

Theoretical and experimental pIs and M_r are also provided. Homologies include the % coverage reached, the number of matched and unmatched peptides, and the Mascot score details. Scores >76 are significant ($P < 0.05$)

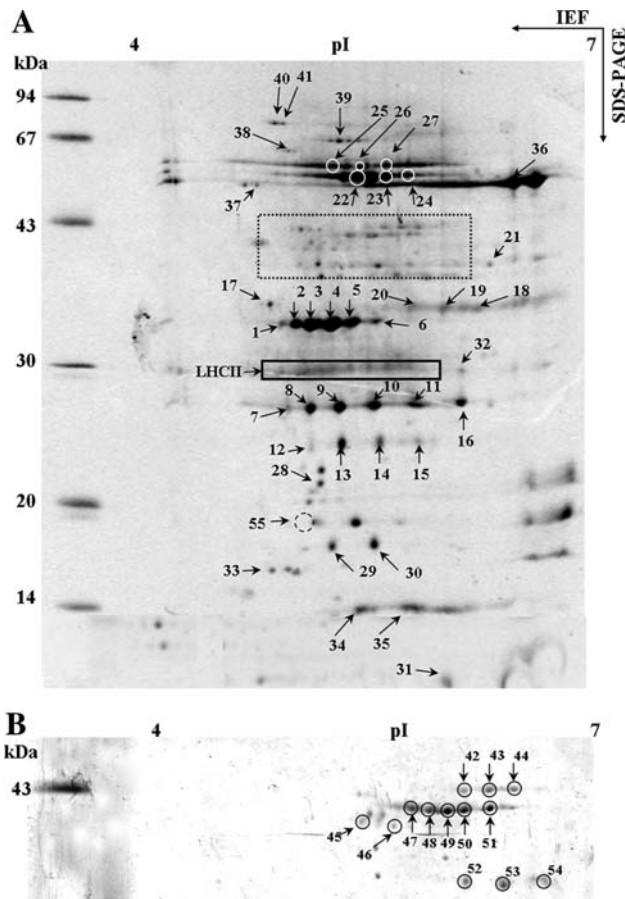


Fig. 1 **a** Sypro-stained 2-DE maps of chloroplast preparations from control *Nicotiana benthamiana* plants. Proteins were separated in the first dimension in linear (pH 4–7) IPG gel strips and in the second dimension in 12% polyacrylamide vertical gels. Identified spots by means of MALDI/TOF-TOF are listed in Table 1. LHCII proteins were detected by Western Blot analysis. The region enclosed by a dotted box is shown in detail in **B**. **b** Detail of the map in the pH 4–7 range, where proteins from # 42 to # 54 have better resolution

high M_r range of the gels with a pI of 6.9, and RbcS (RuBisCO small subunit) in the low M_r range with two spots, showing the same M_r but different pIs (# 34 and 35). We also detected other proteins from the same metabolic pathway: sedoheptulose-1,7-biphosphatase (SBPase, # 45), phosphoribulokinase (PRK, # 46), RuBisCO activase (Rca, # 47–50), phosphoglycerate kinase (PGK, # 49–51), and chloroplastic sedoheptulose/fructose-bisphosphate aldolase (SFBA, # 52–54). Spots 49 and 50 contained a combination of two proteins: Rca and PGK. Other proteins identified corresponded to enzymes of the nitrogen metabolism (glutamine synthetase, GS, # 42–44).

Some proteins linked with stress processes were found in the gels: a RuBisCO-binding chaperonin (# 38), heat shock 70 kDa protein (Hsp70, # 40–41) and the FtsH-like protein (# 39), related to the D1 turnover and to the hypersensitive response in incompatible host–pathogen

interactions. In addition, three proteins with unknown functions were present in the gels: hypothetical protein (# 37), thylakoid luminal 16.5 kDa protein (# 33), and a plastid-lipid-associated protein (# 17).

Chloroplast proteome of control *Nicotiana benthamiana* plants in the pH range 6–11

In the 2-DE map of chloroplastic proteins separated in the basic range, 53 spots appeared (Fig 2). All of these were analyzed by MALDI-TOF/TOF. Only 28 spots could be identified: seven spots corresponded to the pI standards (Table 2) and 21 spots were chloroplastic proteins (Table 1, spots # 56–71). Due to the overlap between acidic (pH 4–7) and basic (pH 6–11) pH ranges, some proteins present in the acid 2-DE map also appeared in the basic one: PsbP from the OEC (# 16), the Cyt. f (# 18) the γ subunit of CF₁ (# 21), Lhca (# 32) and RbcL (# 36). In the overlapping range (6–7) also appears a chlorophyll a/b binding protein from PSII (Lhcb; # 71) not identified in the acidic-range gels. New polypeptides corresponding to

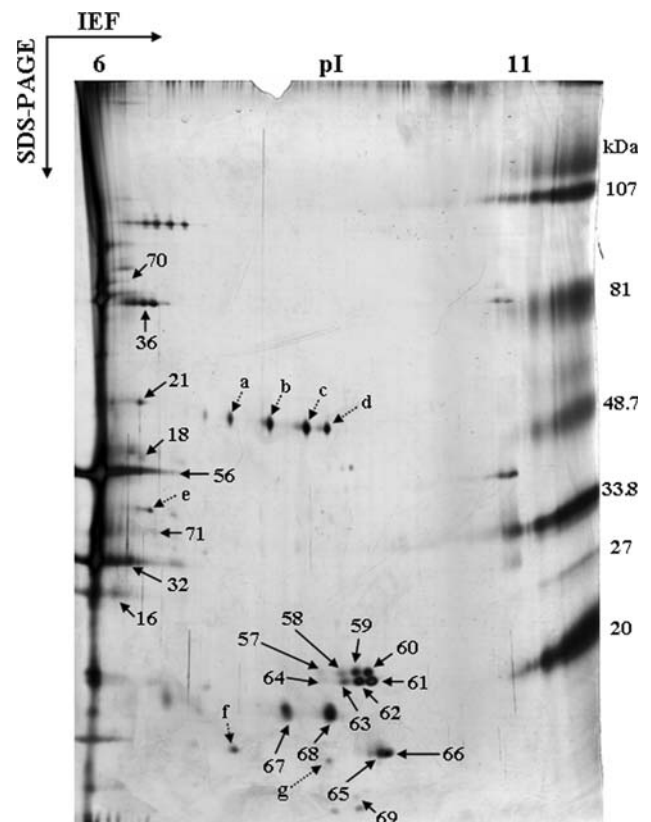


Fig. 2 Silver-stained 2-DE maps of chloroplast preparations from control *Nicotiana benthamiana* plants. Proteins were separated in the first dimension in linear (pH 6–11) IPG gel strips and in the second dimension in 12% polyacrylamide vertical gels. Identified spots by means of MALDI/TOF-TOF are listed in Table 1. Dotted arrows represent pI standards, indicated by letters and listed in Table 2

proteins already identified in the acidic range appeared in the 6–7 pH range: Cyt. f (# 56) and CF₁ α subunit (# 70).

The other proteins identified in the pH range 6–11 were: two spots for the E subunit of PSI (PsaE) with the same M_r and different pI (# 67 and 68); eight spots corresponding to D subunit of PSI (PsaD), four of these with similar M_r and differing in pI (# 57–60); and 4 PsaD proteins with lower M_r (# 61–64). The PsbQ protein from the OEC was detected in the low M_r region of the gel, matching two spots (# 65 and 66). The ribosomal protein L14 was the lowest M_r identified protein (# 69).

Comparative analysis of chloroplast proteomes from control and PMMoV-S infected plants in both pH ranges

Comparative analysis of 2-DE gels from control and PMMoV-S infected *N. benthamiana* plants at 14 dpi (Fig. 3; Table 3), enabled us to identify some proteins that were down-regulated by the viral infection (difference more than 30%, according to “Materials and methods” section) in the pH range 4–7: Cyt. f (# 18 and 20), FNR (# 19), δ and ϵ subunits of CF₁ (# 28–30), RbcL (# 36), RbcS (# 34 and 35), hypothetical protein (# 37), GS (# 42–44), SBPase (# 45), PRK (# 46), Rca (# 47–50), PGK (# 49–51), Lhca (# 32), and SFBA (# 52–54). These are involved in the photosynthetic electron-transport chain, the Benson–Calvin cycle, and nitrogen metabolism. Only one new protein appeared in the chloroplast from infected plants: the viral-coat protein (CP; # 55) with a M_r and pI of 17.6 kDa and 5.2, respectively. Other down-regulated proteins during pathogenesis were detected in the basic range 2D gels: PsaD forms and the ribosomal protein L14 (# 57–64, and 69).

Discussion

Two-dimensional gel electrophoresis has been successfully applied to the analysis of the chloroplast proteome, and especially to the peripheral and luminal one in plants such as *Arabidopsis* and *P. sativum* (Kieselbach et al. 2000; Peltier et al. 2000; van Wijk 2001; Whitelegge 2003). Only a few authors have investigated changes in the chloroplast proteome under abiotic or biotic stress: Andaluz et al. (2006) and Timperio et al. (2007) analyzed the effect of iron deficiency in *B. vulgaris* and *Spinacea oleracea*, respectively; Cui et al. (2005) investigated the impact of cold stress in *O. sativa*; Jones et al. (2006) evaluated changes in the chloroplast proteome of *Arabidopsis* plants infected with *P. syringae* pv. *tomato*; Díaz-Vivancos et al. (2008) showed that changes in the expression levels of proteins from the electron-transport chain correlated with

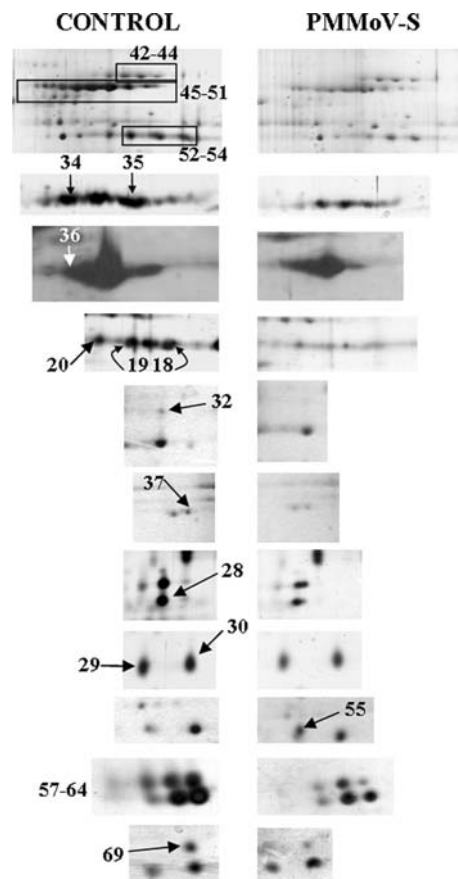


Fig. 3 Changes detected by 2-DE in the expression levels of different chloroplastidic proteins. Left panels correspond to control plants and right panels to PMMoV-S infected plants. All the proteins (excepting # 55, the coat protein of PMMoV-S) present lower expression levels in infected plants. Numbers correspond to those of Table 1. Spots from 1 to 55 are located in the pH range 4–7 gels (Sypro Ruby-stained), while proteins from 56 to 71 are placed in pH range 6–11 gels (silver-stained)

the appearance of reactive oxygen species during the infection of *P. sativum* with *Plum pox virus*.

Also, we performed a proteomic analysis of the OEC from *N. benthamiana* infected with PMMoV (Pérez-Bueno et al. 2004), finding that the OEC proteins were the most abundant ones in the chloroplast proteome. Previously, we had described them as a target of infection with this tobamovirus (Rahoutei et al. 1998). In the present study, we go further into the analysis of the chloroplast proteome of *N. benthamiana* at 14 dpi using 2-DE and MS followed by database searching. At 14 dpi, the effects of PMMoV-S infection in *N. benthamiana* plants are highly significant, as evaluated by visual symptoms (Pineda et al. 2008b), lower mRNA levels of chloroplastidic proteins (Pérez-Bueno 2003), imbalance of ATP + NADPH assimilatory potential (Sajnani et al. 2007), alterations in fluorescence emissions (Pineda et al. 2008a, b), and stomatal closure (Chaerle et al. 2006).

Table 3 Content of chloroplastic proteins from PMMoV-S infected plants relative to the controls (averages \pm standard deviation)

Spot	Homology	Relative content (%)
18	Cyt. f	82.8 \pm 3.6
19	FNR, chain b	78.9 \pm 4.0
20	Cyt. f	61.0 \pm 2.0
28	CF1 δ	55.0 \pm 4.1
29	CF1 ϵ	42.0 \pm 3.0
30	CF1 ϵ	31.3 \pm 0.9
32	Lhca Type III	60.5 \pm 6.5
34	RbcS	46.3 \pm 2.2
35	RbcS	74.6 \pm 1.6
36	RbcL	40.4 \pm 5.4
37	Hypothetical protein	61.2 \pm 6.2
42	GS	54.6 \pm 2.8
43	GS	40.6 \pm 2.4
44	GS	40.4 \pm 3.6
45	SBPase	59.8 \pm 4.5
46	PRK	71.2 \pm 5.6
47	Rca	71.5 \pm 1.6
48	Rca	66.9 \pm 2.8
49	PGK	55.1 \pm 6.7
	Rca	
50	PGK	72.9 \pm 6.8
	Rca	
51	PGK	73.6 \pm 3.3
52	SFBA	75.6 \pm 0.5
53	SFBA	60.5 \pm 4.0
54	SFBA	36.2 \pm 3.9
55	CP	100 \pm 0.0
57	PsaD	78.3 \pm 1.4
58	PsaD	66.3 \pm 1.5
59	PsaD	47.6 \pm 1.1
60	PsaD	86.9 \pm 2.0
61	PsaD	43.2 \pm 4.0
62	PsaD	31.5 \pm 1.2
63	PsaD	34.9 \pm 2.9
64	PsaD	77.1 \pm 2.6
69	Ribosomal protein L14	66.3 \pm 6.7

Proteins were isolated by 2-DE gels (Figs. 1, 2) and identified by MALDI/TOF-TOF

CF₁, ATP synthase catalytic portion; CP, viral-coat protein; Cyt. f, cytochrome f; FNR, ferredoxin-NADP⁺ reductase; GS, glutamine synthetase; Lhca, PSI chlorophyll a/b binding proteins; PGK, phosphoglycerate kinase; PRK, phosphoribulo-kinase; Psa proteins, PSI proteins codified by *psa* genes; RbcL, RuBisCO large subunit; RbcS, RuBisCO small subunit; Rca, RuBisCO activase; SBPase, sedoheptulose-1,7-bisphosphatase; SFBA, sedoheptulose/fructose-bisphosphate aldolase

More than 200 spots were visualized in the 2-DE gel from chloroplast preparations isolated from control plants: 150 spots in the pH range 4–7, mostly in the 20–43 kDa M_r

region (Fig. 1a, b), and 53 spots in the pH range 6–11 (Fig. 2). From the MALDI-TOF/TOF analysis, 71 proteins were identified; in addition, several LHCII proteins were identified by Western Blot (Fig. 1a, data not shown). The 2-DE gels showed that proteins involved in carbon fixation were still present in our preparations after removing the stromal fraction. However, some authors have already found evidence that Benson–Calvin cycle enzymes can assemble into stable multi-enzyme complexes bound to the stromal face of thylakoid membranes in different plant species (Rodríguez Andrés et al. 1987; Gontero et al. 1988; Süß et al. 1993, 1995; Anderson et al. 1996; Andaluz et al. 2006), including *N. tabacum* (Jebanathirajah and Coleman 1998). This kind of association has been proposed to grant direct access to required cofactors such as ATP and NADPH, and to prevent interferences by other metabolic pathways (Süß et al. 1993; Anderson et al. 1996).

Particularly remarkable was the high number of PsbO and PsbP spots, 6 and 10, respectively (Fig. 1a; Table 1). We have previously identified four isoforms of each protein family (Rahoutei et al. 1998; Pérez-Bueno et al. 2004), both encoded by a multigene family with at least four isogenes (Pérez-Bueno 2003). PsbO protein families have been described in *P. sativum* (Wales et al. 1989), *Lycopersicon esculentum* (Görlach et al. 1993) and *A. thaliana* (Kieselbach et al. 2000; Peltier et al. 2002; Schubert et al. 2002). PsbP protein families were found in *Nicotiana tabacum* (Hua et al. 1991a, b; Takahashi et al. 1991; Hua et al. 1993), *A. thaliana* (Peltier et al. 2002) and *Sinapis alba* (Merkle et al. 1990). It has been demonstrated in *N. tabacum* that the four PsbP isoforms are functionally equivalent in vivo, but the expression of the four isogenes is required for optimal PSII activity (Ishihara et al. 2005). We have also demonstrated that the expression level of the various PsbP isoforms is differentially affected by the PMMoV infection in *N. benthamiana* (Pérez-Bueno et al. 2004). Analysis of the two PsbO isogenes from *A. thaliana* revealed that they were not equivalent; the down-regulation of the expression from every isogene induced that of other PSII proteins and a reduced activity of this photosynthetic complex (Murakami et al. 2005).

The higher number of PsbP and PsbO spots found in this study compared with our previous findings (Pérez-Bueno et al. 2004), could be because, in our earlier experiments, we used self-made disk gels for the IEF, whereas, in the present study, we carried out the IEF using ready-made IPG Strip gels. This technique allows higher resolution, more reproducible patterns and better focusing of the basic proteins (Corbett et al. 1994; Görg et al. 2000). From the six and ten spots detected for the PsbO and PsbP proteins, respectively, some may have been the result of post-transcriptional alterations, given that we have found only four isogenes codifying each protein family (Pérez-Bueno

2003). Further analysis of these spots carried out by electrospray ionization-MS will clarify this point.

The reported fall in the levels of PsbP isoforms due to the viral infection (Pérez-Bueno et al. 2004) was not evident in the present acidic 2-DE maps. With the OEC proteins being the most prominent ones in this pH range, the PsbO and PsbP signals were saturated (Fig. 1a), because we loaded a high amount of protein in these gels in order to identify minor proteins in the *N. benthamiana* chloroplast proteome.

In the alkaline 2-DE map (pH 6–11), we detected two spots for the PsbQ protein (pI 9.4 and 9.5; Fig. 2 and Table 1), in accordance with the two *psbQ* isogenes that we have reported previously for *N. benthamiana* (Pérez-Bueno 2003). Two PsbQ isoforms were identified by 2-DE on *A. thaliana* chloroplast preparations (Kieselbach et al. 2000; Schubert et al. 2002), while Peltier et al. (2000) detected only one spot in 2-DE gels from *P. sativum* chloroplasts.

The different subunits of the CF₁, together with the OEC proteins, are the most abundant polypeptides in the acidic pH range (Fig. 1a, b). These data agree with the 2-DE maps from the thylakoid proteome of *A. thaliana* investigated by Friso et al. (2004). In our gels, all subunits of the CF₁ fragment from the ATP synthase were found. Due to the analogy with Friso et al. (2004) gels, we propose that proteins with the same M_r close to CF₁ α and CF₁ β (Fig. 1a) would be protein trains of these subunits.

We also identified several high M_r chaperonins (Fig. 1; Table 1): the 60-kDa chaperonin, participating in RuBisCO assembly (Buchanan et al. 2000) and Hsp70, involved in PSII stress protection (Schroda et al. 2001). The FtsH-like related to PSII repair and turnover (Nixon et al. 2005; Cheregi et al. 2005; Zaltsman et al. 2005a, b) was also present in the 2-DE gels. Two of the spots identified in our 2-DE maps (hypothetical protein and the thylakoid luminal 16.5 kDa proteins) have unknown functions; the hypothetical protein amount decreased in the plants infected with PMMoV-S (Fig. 3; Table 3).

Comparative analysis of the chloroplastidic proteome from control and PMMoV-S infected plants at 14 dpi revealed that the expression levels of some proteins implicated in Benson–Calvin cycle, electron-transport chain and nitrogen metabolism decreased during the PMMoV-S infection (Fig. 3; Table 3).

The proteins involved in the Benson–Calvin cycle affected by the PMMoV infection are: RbcL, RbcS, Rca, SFBA, SBPase, PGK, and PRK (Fig. 3; Table 3). The decrease in the amounts of these polypeptides is consistent with the lower transcript levels of these proteins during viral and bacterial pathogenesis (Pérez-Bueno 2003; Ishiga et al. 2009, respectively). The degradation of the RbcL subunit under different stress conditions (UV radiation, ozone, and osmotic, etc.) is for some authors a

consequence of oxidative alterations in this enzyme (Houtz et al. 2003 and references therein). Oxidative stress is usually induced in infected plants (Foyer and Harbinson 1994; Vranová et al. 2002). The Rca has a dual function: activating the RuBisCO complex; and, as a chaperonin, protecting protein synthesis under stress conditions (Sánchez de Jiménez et al. 1995; Rokka et al. 2001). SFBA is codified by two genes in *Nicotiana* with differential expression levels under salt stress (Yamada et al. 2000). A similar situation seems to occur in our PMMoV-S infected plants. We have identified three protein spots corresponding to SFBA, with number 52 being the most affected by the PMMoV-S infection. Probably, the additional spot is due to post-translational modifications. In order to evaluate the impact of the lower levels of the SBPase (this being one of the key regulatory enzymes of the Benson–Calvin cycle) and PRK in infected plants, we take as model a transgenic plant showing different expression levels of both enzymes. Decreases on SBPase amounts limit CO₂ fixation and leaf carbohydrate content (Harrison et al. 1998), while the overexpression of this enzyme enhances photosynthesis against high-temperature stress in transgenic rice plants (Feng et al. 2007). In general, it is well documented that the fall in the levels of Benson–Calvin enzymes induced adverse effects on CO₂ fixation, photosynthesis rate, carbohydrates accumulation, and plant growth (Haake et al. 1998; Banks et al. 1999; Raines 2003). We have also documented a decrease of the net photosynthesis rate of the host plant under infection with PMMoV (Pineda et al. 2008b); a similar situation was found by Zhou et al. (2006) and Ishiga et al. (2009) during bacterial challenge.

The plastid GS, a key protein in the nitrogen metabolism, is also diminished in plants infected by PMMoV-S (Fig. 3; Table 3). Senescent plants show also a fall in both protein and mRNA levels of this enzyme, whereas, the cytosolic one is induced (Masclaux-Daubresse et al. 2005; Teixeira et al. 2005). PMMoV-S infection on *N. benthamiana* shows similarities with senescence processes. In clover (*Trifolium repens* L.), senescence lowers levels of PsbO, both RuBisCO subunits and Rca, as well as GS (Wilson et al. 2002). This down-regulation pattern is similar to that found in symptomless leaves of PMMoV-infected *N. benthamiana* plants for the transcripts of these proteins (Pérez-Bueno 2003), confirming that viral infection accelerates senescence processes.

With respect to electron-transport chain proteins, in the 2-DE maps of the alkaline pH range from *N. benthamiana* chloroplasts, some PSI proteins appeared, such as the Psd and PsaE (Fig. 2; Table 1). These highly hydrophilic proteins, together with PsaC, which could be distinguished in gels within a low pH range (Fig. 1a; Table 1), are located on the PSI stromal side, being involved in the ferredoxin-docking (Sétif et al. 2002). Psd and PsaE are codified by

nuclear genes, two isogenes for both existing in *A. thaliana* (Naver et al. 1999; Ihnatowicz et al. 2004) and *Nicotiana* spp. (Obokata et al. 1993, 1994; Yamamoto et al. 1993). In the case of *Nicotiana sylvestris*, the two *psaE* isogenes codify for four different polypeptides; however, we could detect only two PsaE spots in *N. benthamiana*. In *N. sylvestris*, PsaD is also a protein family with two isoforms (PsaD1 and PsaD2), functionally redundant, encoded by two isogenes. Nevertheless, we detected up to eight PsaD spots, the expression levels of which diminished due to the viral infection (Figs. 2, 3; Table 3). Because of the high homology between PsaD1 and PsaD2 proteins (96/95% similarity/identity, Ihnatowicz et al. 2004), they could not be distinguished by the MALDI-TOF/TOF analysis. The *psaD* genes are differentially expressed during leaf development in *N. sylvestris* (Yamamoto et al. 1993). *Arabidopsis* PsaD double mutants showed that this protein is essential for photosynthesis (Ihnatowicz et al. 2004). Its down-regulation induces both a high non-photochemical quenching and steady-state chlorophyll fluorescence (Haldrup et al. 2003) as well as a decrease in linear PSI electron-transport activity (Montesano et al. 2004); a similar phenomenon was observed in our PMMoV-infected plants (Chaerle et al. 2006; Pérez-Bueno et al. 2006; Sajjani et al. 2007; Pineda et al. 2008a, b). Other authors have also shown that the PsaD content decreases in Fe-deficient *Arabidopsis* plants (Laganowsky et al. 2009).

Other proteins from the electron-transport chain with expression levels diminished due to the PMMoV-S infection are Cyt. f, FRN, and some polypeptides belonging to the light-harvesting complexes from both photosystems (Fig. 3; Table 3), according to the recent results for Fe-deficient *Arabidopsis* plants (Laganowsky et al. 2009). While we detected only one spot corresponding to FNR, several isoforms of this oxidoreductase have been found in other plants. In *Arabidopsis* (two isoforms) and maize (three isoforms), FNR isoproteins are believed to play different roles in response to the nitrogen regime (Hanke et al. 2005; Okutani et al. 2005, respectively), whereas in wheat the two present isoforms may substitute for each other under certain physiological conditions (Grzyb et al. 2008). It is unknown how many genes code for FNR in tobacco (Lintala et al. 2007). Transgenic tobacco plants overexpressing FNR exhibited enhanced tolerance to photo-oxidative damage (Rodríguez et al. 2007), while lower activity of this protein in the chloroplast leads to impaired plant growth and restricts photosynthesis capacity (Hajirezaei et al. 2002). The impact of the PMMoV infection on the photosynthetic electron transport described in our previous studies (Rahoutei et al. 2000; Pérez-Bueno et al. 2004), could be explained by the down-regulation of proteins involved in this photosynthetic step as well as in light harvesting.

Another chloroplastidic protein present in the alkaline pH range and affected by the PMMoV-S infection is the ribosomal protein L14 (Fig. 3; Table 3), a protein from the chloroplastidic large ribosomal subunit (Tanaka et al. 1986). The significance of its decrease in PMMoV-S-infected plants remains unclear.

The presence of multigene families for different chloroplastidic proteins—PsbO, PsbP, PsbQ, PsaD, PsaE, and SFBA—in *N. benthamiana* appear to enable the host plant to react in a more flexible way to environmental stimuli and different stress factors (Koiwa et al. 2002).

The understanding of the chloroplast proteome of *N. benthamiana*, a promiscuous host for different viral families, is of high interest for the study of the virus–plant interactions. Despite its limitations, the 2-DE technique was powerful enough to generate maps with about 200 polypeptides. Taking into account that the *N. benthamiana* genome is not completely sequenced, we identified a high number of proteins, similar to the number reported in other publications cited above. The future applications of non-gel-proteomic techniques for the study of the *N. benthamiana* chloroplastidic proteome, together with the progress in sequencing the genome of this host plant, will help to enlarge an emerging investigation field lacking in these types of studies: the influence of biotic-stress factors in the proteome of the photosynthetic apparatus.

Acknowledgments This research was supported by grants from the Spanish Government (BIO2004-04968-C02-02, BIO2007-67874-C02-02 and AGL2008-00214 to M.B.) and FEDER Funds. The authors are very grateful to Drs. Isabel García Luque and Maite Serra (Centro Investigaciones Biológicas, CSIC, Madrid) for providing all PMMoV solutions and antibodies against the viral-coat protein. In addition, they thank J.A. López, E. Camafeita and E. Calvo from the Proteomic Unit of the National Centre for Cardiovascular Research (Madrid, Spain) for the skilful assistance with the MALDI/TOF-TOF analysis and protein identification.

References

- Alonso E, García-Luque I, Ávila-Rincón MJ, Wicke B, Serra MT, Díaz-Ruiz JR (1989) A tobamovirus causing heavy losses in protected pepper crops in Spain. *J Phytopathol* 125:67–76
- Andaluz S, López-Millán AF, De Las Rivas J, Aro EM, Abadía J, Abadía A (2006) Proteomic profiles of thylakoid membranes and changes in response to iron deficiency. *Photosynth Res* 89:141–155
- Anderson LE, Gibbons JT, Wang X (1996) Distribution of ten enzymes of carbon metabolism in pea (*Pisum sativum*) chloroplasts. *Int J Plant Sci* 157:525–538
- Aro EM, Soursa M, Rokka A, Allahverdiyeva Y, Paakkarinen V, Saleem A, Battchikova N, Rintamaki E (2005) Dynamics of photosystem II a proteomic approach to thylakoid protein complexes. *J Exp Bot* 56:347–356
- Bagginsky S, Gruissem W (2004) Chloroplast proteomics: potentials and challenges. *J Exp Bot* 400:1213–1220
- Banks FM, Driscoll SP, Parry MAJ, Lawlor DW, Knight JS, Gray JC, Paul MJ (1999) Decrease in phosphoribulokinase activity by

- antisense RNA in transgenic tobacco. Relationship between photosynthesis, growth and allocation at different nitrogen levels. *Plant Physiol* 119:1125–1136
- Buchanan BB, Wilhelm G, Jones RL (2000) Biochemistry and molecular biology of plants. American Society of Plant Biologist, Rockville
- Cánovas FM, Dumas-Gaudot E, Recorbet G, Jorrín JV, Mock H-P, Rossignol M (2004) Plant proteome analysis. *Proteomics* 4:285–298
- Chaerle L, Pineda M, Romero-Aranda R, Van Der Straeten D, Barón M (2006) Robotized thermal and chlorophyll fluorescence imaging of pepper mild mottle virus infection in *Nicotiana benthamiana*. *Plant Cell Physiol* 47:1323–1336
- Cherei O, Sicora C, Kos PB, Nixon PJ, Vass I (2005) The FtsH protease is required for the repair of photosystem II in the cyanobacterium *Synechocystis* 6803 damaged by UV-B radiation. *BMC Plant Biol* 5: S8. (Meeting abstract)
- Ciambella C, Roepstorff P, Aro EM, Zolla L (2005) A proteomics approach for investigation of photosynthetic apparatus in plants. *Proteomics* 5:746–757
- Corbett JM, Dunn MJ, Posch A, Görg A (1994) Positional reproducibility of protein spots in two-dimensional polyacrylamide gel electrophoresis using immobilized pH gradient isoelectric focusing in the first dimension: an interlaboratory comparison. *Electrophoresis* 15:1205–1211
- Cui S, Huang F, Wang J, Ma X, Cheng Y, Liu J (2005) A proteomic analysis of cold stress responses in rice seedlings. *Proteomics* 5:3162–3172
- Curto M, Camafeita E, López JA, Maldonado AM, Rubiales D, Jorrín JV (2006) A proteomic approach to study pea (*Pisum sativum*) responses to powdery mildew (*Erysiphe pisi*). *Proteomics* 6:S163–S174
- Díaz-Vivancos P, Clemente-Moreno M, Rubio M, Olmos E, García JA, Martínez-Gómez P, Hernández JA (2008) Alteration in the chloroplastic metabolism leads to ROS accumulation in pea plants in response to *Plum pox virus*. *J Exp Bot* 59:2147–2160
- Feng L, Wag K, Li Y, Tan Y, Kong J, Li H, Li Y, Zhu Y (2007) Overexpression of SBPase enhances photosynthesis against high temperature stress in transgenic rice plants. *Plant Cell Rep* 26:1635–1646
- Ferro M, Salvi D, Rivière-Rolland H, Vermet T, Seigneurin-Berny D, Grunwald D, Garin J, Joyard J, Rolland N (2002) Integral membrane proteins of the chloroplast envelope: identification and subcellular localization of new transporters. *Proc Natl Acad Sci USA* 99:11487–11492
- Foyer CH, Harbinson J (1994) Oxygen metabolism and the regulation of photosynthetic electron transport. In: Foyer CH, Mullineaux PM (eds) Causes of photooxidative stress and amelioration of defense system in plants. CRC Press, Boca Raton
- Friso G, Giacomelli L, Ytterberg JA, Peltier JB, Rudella A, Sun Q, van Wijk KJ (2004) In-depth analysis of the thylakoid membrane proteome of *Arabidopsis thaliana* chloroplasts: new proteins, new functions, and a plastid proteome database. *Plant Cell* 16:478–499
- Giacomelli L, Rudella A, van Wijk KJ (2006) High light response of the thylakoid proteome in *Arabidopsis* wild type and the ascorbate-deficient mutant *vtc2-2*. A comparative proteomics study. *Plant Physiol* 141:685–701
- Gontero B, Cárdenas ML, Ricard J (1988) A functional 5-enzyme complex of chloroplast involved in the Calvin cycle. *Eur J Biochem* 173:437–443
- Görg A, Obermaier C, Boguth G, Harder A, Scheibe B, Wildgruber R, Weiss W (2000) The current state of two-dimensional electrophoresis with immobilized pH gradients. *Electrophoresis* 21:1037–1053
- Görlach J, Schmid J, Amrhein N (1993) The 33 kDa protein of the oxygen-evolving complex: a multi-gene family in tomato. *Plant Cell Physiol* 34:479–501
- Grzyb J, Malec P, Rumak I, Garstka M, Strzalka K (2008) Two isoforms of ferredoxin: NADP⁺ oxidoreductase from wheat leaves: purification and initial biochemical characterization. *Photosynth Res* 96:99–112
- Haake V, Zrenner R, Sonnewald U, Stitt M (1998) A moderate decrease of plastid aldolase activity inhibits photosynthesis, alters the levels of sugars and starch, and inhibits growth of potato plants. *Plant J* 14:147–157
- Hajirezaei MR, Peisker M, Tschiersch H, Palatnik JF, Valle EM, Carrillo N, Sonnewald U (2002) Small changes in the activity of chloroplast NADP⁺-dependent ferredoxin reductase lead to impaired plant growth and restrict photosynthetic capacity of transgenic tobacco plants. *Plant J* 29:281–293
- Haldrup A, Lunde C, Scheller HV (2003) *Arabidopsis thaliana* plants lacking the PSI-D subunit of photosystem I suffer photoinhibition, have unstable photosystem I complexes, and altered redox homeostasis in the chloroplast stroma. *J Biol Chem* 278:33276–33283
- Hanke GT, Okutani S, Satomi Y, Takao T, Suzuki A, Hase T (2005) Multiple iso-proteins of FNR in *Arabidopsis*: evidence for different contributions to chloroplast function and nitrogen assimilation. *Plant Cell Environ* 28:1146–1157
- Harrison EP, Willingham NM, Lloyd JC, Raines CA (1998) Reduced sedoheptulose-1, 7-bisphosphatase levels in transgenic tobacco lead to decreased photosynthetic capacity and altered carbohydrate accumulation. *Planta* 204:27–36
- Houtz RL, AR Jr Portis (2003) The life of ribulose 1, 5-bisphosphate carboxylase/oxygenase—Posttranslational facts and mysteries. *Arch Biochem Biophys* 414:150–158
- Hua SB, Dube SK, Barnett NM, Kung SD (1991a) Nucleotide sequence of a cDNA clone encoding 23 kDa polypeptide of the oxygen-evolving complex of photosystem II in tobacco, *Nicotiana tabacum* L. *Plant Mol Biol* 16:749–750
- Hua SB, Dube SK, Barnett NM, Kung SD (1991b) Nucleotide sequence of gene *oe2-A* and its cDNA encoding 23 kDa polypeptide of the oxygen-evolving complex of photosystem II in tobacco. *Plant Mol Biol* 17:551–553
- Hua SB, Dube SK, Kung SD (1993) Molecular evolutionary of the *psbP* gene family of the photosystem II oxygen-evolving complex in *Nicotiana*. *Genome* 36:483–488
- Huber CG, Walcher W, Timperio A, Troiani S, Porceddu A, Zolla L (2004) Multidimensional proteomic analysis of photosynthetic membrane proteins by liquid extraction-ultracentrifugation-liquid chromatography-mass spectrometry. *Proteomics* 4:3909–3920
- Ihnatowicz A, Pesaresi P, Varotto C, Richly E, Schneider A, Jahns P, Salamini F, Leister D (2004) Mutants for photosystem I subunit D of *Arabidopsis thaliana*: effects on photosynthesis, photosystem I stability and expression of nuclear genes for chloroplast functions. *Plant J* 37:839–852
- Ishiga Y, Uppalapati SR, Ishiga T, Elavarthi S, Martin B, Bender CL (2009) The phytotoxin coronatine induces light-dependent reactive oxygen species in tomato seedlings. *New Phytol* 181:147–160
- Ishihara S, Yamamoto Y, Ifuku K, Sato F (2005) Functional analysis of four members of the PsbP family in photosystem II in *Nicotiana tabacum* using differential RNA interference. *Plant Cell Physiol* 46:1885–1893
- Jebanathirajah JA, Coleman JR (1998) Association of carbonic anhydrase with a Calvin cycle enzyme complex in *Nicotiana tabacum*. *Planta* 204:177–182
- Jones AME, Bennett MH, Mansfield JW, Grant M (2006) Analysis of the defence phosphoproteome of *Arabidopsis thaliana* using differential mass tagging. *Proteomics* 6:4155–4165

- Jorrín JV, Maldonado AM, Castillejo MA (2007) Plant proteome analysis: a 2006 update. *Proteomics* 7:2947–2962
- Jorrín JV, Maldonado AM, Echevarría-Zomeño S, Valledor L, Castillejo MA, Curto M, Valero J, Sghaier B, Donoso G, Redondo I (2009) Plant proteomics update (2007–2008): second-generation proteomic techniques, an appropriate experimental design, and data analysis to fulfil MIAPE standards, increase plant proteome coverage and expand biological knowledge. *J Proteomics* 72:285–314
- Kieselbach T, Hagman A, Andersson B, Schröder PW (2000) The thylakoid lumen of chloroplast. Isolation and characterization. *J Biol Chem* 273:6710–6716
- Kleffman T, Russenberger D, von Zychlinski A, Christopher W, Sjölander K, Gruissem W, Baginsky S (2004) The *Arabidopsis thaliana* chloroplast proteome reveals pathway abundance and novel protein functions. *Curr Biol* 14:354–362
- Koiwa H, Barb AW, Xiong L, Li F, McCully MG, Lee B, Sokolchik I, Zhu J, Gong Z, Reddy M, Sharkhuu A, Manabe Y, Yokoi S, Zhu JK, Bressan RA, Hasegawa PM (2002) C-terminal domain phosphatase-like family members (AtCPLs) differentially regulate *Arabidopsis thaliana* abiotic stress signalling, growth, and development. *Proc Natl Acad Sci* 99:10893–10898
- Laganowsky A, Gómez SM, Whitelegge JP, Nishio JN (2009) Hydroponics on a chip: analysis of the Fe deficient *Arabidopsis thaliana* thylakoid membrane proteome. *J Proteomics* 72:397–415
- Lintala M, Allahverdiyeva Y, Kidron H, Piippo M, Battchikova N, Suorsa M, Rintamäki E, Salminen TA, Aro E-M, Mulo P (2007) Structural and functional characterization of ferredoxin-NADP⁺-oxidoreductase using knock-out mutants of *Arabidopsis*. *Plant J* 49:1041–1052
- Masclaux-Daubresse C, Carrayol E, Valadier MH (2005) The two nitrogen mobilisation- and senescence-associated GS1 and GDH genes are controlled by C and N metabolites. *Planta* 221: 580–588
- Merkle TH, Krenz M, Weng A, Schäfer E (1990) Nucleotide sequence and deduced amino acid sequence of a gene encoding the 23 kDa polypeptide of the oxygen-evolving complex from mustard (*Sinapis alba* L). *Plant Mol Biol* 14:889–890
- Montesano M, Scheller HV, Wettstein R, Palva ET (2004) Down-regulation of photosystem I by *Erwinia carotovora*-derived elicitors correlates with H₂O₂ accumulation in chloroplasts of potato. *Mol Plant Pathol* 5:115–123
- Murakami R, Ifuku K, Takabayashi A, Shikanai T, Endo T, Sato F (2005) Functional dissection of two *Arabidopsis* PsbO2. *FEBS J* 272:2165–2175
- Naver H, Haldrup A, Scheller HV (1999) Cosuppression of photosystem I subunit PSI-H in *Arabidopsis thaliana*. Efficient electron transfer and stability of photosystem I is dependent upon the PSI-H subunit. *J Biol Chem* 274:10784–10789
- Newton RP, Brenton AG, Smith CJ, Dudley E (2004) Plant proteome analysis by mass spectrometry: principles, problems, pitfalls and recent developments. *Phytochemistry* 65:1449–1485
- Nixon PJ, Barker M, Boehm M, de Vries R, Komenda J (2005) FtsH-mediated repair of the photosystem II complex in response to light stress. *J Exp Bot* 56:357–363
- Obokata J, Mikami K, Hayashida N, Nakamura M, Sugiera M (1993) Molecular heterogeneity of photosystem I. psaD, psaE, psaF, psaH and psaL are all present in isoforms in *Nicotiana* spp. *Plant Physiol* 102:1259–1267
- Obokata J, Mikami K, Yamamoto Y, Hayashida N (1994) Microheterogeneity of PSI-E subunit of photosystem I in *Nicotiana sylvestris*. *Plant Cell Physiol* 35:203–209
- Okutani S, Hanke GT, Satomi Y, Takao T, Kurisu G, Suzuki A, Hase T (2005) Three maize leaf ferredoxin:NADP(+) oxidoreductase vary in subchloroplast location, expression, and interaction with ferredoxin. *Plant Physiol* 139:1451–1459
- Peltier JB, Friso G, Kalume ED, Roepstorff P, Nilsson F, Adamska I, van Wijk KJ (2000) Proteomics of the chloroplasts: systematic identification and targeting analysis of luminal and peripheral thylakoid proteins. *Plant Cell* 12:319–341
- Peltier JB, Emanuelsson O, Kalume DE, Ytterberg J, Friso G, Rudella A, Liberles DA, Söderberg L, Roepstorff P, von Heijne G, van Wijk KJ (2002) Central functions of the luminal and peripheral thylakoid proteome of *Arabidopsis* determined by experimentation and genome-wide prediction. *Plant Cell* 14:211–236
- Peltier JB, Ytterberg JA, Sun Q, van Wijk KJ (2004) New functions of the thylakoid membrane proteome of *Arabidopsis thaliana* revealed by a simple, fast, and versatile fractionation strategy. *J Biol Chem* 279:49367–49383
- Pérez-Bueno ML (2003) Photosystem II and viral infection: analysis of fluorescence imaging and regulation of the synthesis of the oxygen-evolving-complex proteins during pathogenesis. Ph. D. Thesis, Granada University, Spain
- Pérez-Bueno ML, Rahoutei J, Sajani C, García-Luque I, Barón M (2004) Proteomic analysis of the oxygen-evolving complex of photosystem II under biotic stress. Studies on *Nicotiana benthamiana* infected with tobamoviruses. *Proteomics* 4: 418–425
- Pérez-Bueno ML, Ciscato M, vandeVen M, García-Luque I, Valcke R, Barón M (2006) Imaging viral infection. Studies on *Nicotiana benthamiana* plants infected with the pepper mild mottle tobamovirus. *Photosynth Res* 90:111–123
- Phee B-K, Cho J-H, Park S, Jung JH, Lee Y-H, Jeong J-S, Bhoo SH, Hahn T-R (2004) Proteomic analysis of the response of *Arabidopsis* chloroplast proteins to high light stress. *Proteomics* 4:3560–3568
- Pineda M, Gáspár L, Morales F, Szigeti Z, Barón M (2008a) Multicolour fluorescence imaging: a useful tool to visualise systemic viral infections in plants. *Photochem Photobiol* 84:1048–1060
- Pineda M, Soukupová J, Matouš K, Nedbal L, Barón M (2008b) Conventional and combinatorial chlorophyll fluorescence imaging of tobamovirus-infected plants. *Photosynthetica* 46:441–451
- Rahoutei J, García-Luque I, Cremona V, Barón M (1998) Effect of tobamovirus infection on PSII complex of infected plants. In: Garab G (ed) *Photosynthesis: from light to biosphere*. Kluwer, Dordrecht
- Rahoutei J, García-Luque I, Barón M (2000) Inhibition of photosynthesis by viral infection: effect on PSII structure and function. *Physiol Plant* 110:286–292
- Raines CA (2003) The Calvin cycle revisited. *Photosynth Res* 110:286–292
- Reche A, Lázaro JJ, Hermoso R, Chueca A, López Gorgé J (1997) Binding and activation of pea chloroplast fructose-1, 6-bisphosphatase by homologous thioredoxins m and f. *Physiol Plantarum* 101:463–470
- Rodríguez Andrés A, Lázaro JJ, Chueca A, Hermoso R, López Gorgé J (1987) Binding of photosynthetic fructose-1, 6-bisphosphatase to chloroplast membranes. *Plant Sci* 52:41–48
- Rodríguez RE, Lodeyro A, Poli HO, Zurbriggen M, Peisker M, Palatnik JF, Tognetti VB, Tschiersch H, Hajirezaei MR, Valle EM, Carrillo N (2007) Transgenic tobacco plants overexpressing chloroplastic ferredoxin-NADP(H) reductase display normal rates of photosynthesis and increased tolerance to oxidative stress. *Plant Physiol* 143:639–649
- Rokka A, Zhang L, Aro EM (2001) RuBisCO activase: an enzyme with a temperature-dependent dual function? *Plant J* 25:463–471
- Rose JK, Bashir S, Giovannoni JJ, Jahn MM, Saravanan RS (2004) Tackling the plant proteome: practical approaches, hurdles and experimental tools. *Plant J* 39:715–733
- Rosignol M (2001) Analysis of the plant proteome. *Curr Opin Biotech* 12:131–134

- Rossignol M, Peltier J-B, Mock H-P, Matros A, Maldonado AM, Jorrín JV (2006) Plant proteome analysis: a 2004–2006 update. *Proteomics* 6:5529–5548
- Sajani C, Zurita JL, Roncel M, Ortega JM, Barón M, Ducruet J-M (2007) Changes in photosynthetic metabolism induced by tobamovirus infection in *Nicotiana benthamiana* studied in vivo by thermoluminescence. *New Phytol* 175:120–130
- Sánchez de Jiménez E, Medrano L, Martínez-Barajas E (1995) RuBisCO-activase, a possible new member of the molecular chaperone family. *Biochemistry* 34:2826–2831
- Schägger H, Cramer WA, von Jagow G (1994) Analysis of molecular masses and oligomeric states of protein complexes by blue native electrophoresis and isolation of membrane protein complexes by two-dimensional native electrophoresis. *Anal Biochem* 217:220–230
- Schevchenko A, Wilm M, Vorm O, Mann M (1996) Mass spectrometric sequencing of proteins from silver stained polyacrylamide gels. *Anal Chem* 68:850–858
- Schroda M, Kropat J, Oster U, Rudiger W, Vallon O, Wollman FA, Beck CF (2001) Possible role for molecular chaperones in assembly and repair of photosystem II. *Biochem Soc Trans* 29:413–418
- Schubert M, Petersson UA, Haas BJ, Funk C, Schöder WP, Kieselbach T (2002) Proteome map of the chloroplast lumen of *Arabidopsis thaliana*. *J Biol Chem* 277:8354–8365
- Schuster AM, Davies E (1983) Ribonucleic acid and protein metabolism in pea epicotyls. *Plant Physiol* 73:809–816
- Sétif P, Fischer N, Lagoutte B, Bottin H, Rochaix J-D (2002) The ferredoxin docking site of photosystem I. *Biochim Biophys Acta* 1555:204–209
- Steinberg TH, Jones LJ, Haugland RP, Singer VL (1996) SYPRO Orange and SYPRO Red Protein gel stains: one-step fluorescent staining of denaturing gels for detection of nanogram levels of protein. *Anal Biochem* 239:223–237
- Suckau D, Resemann A, Schuereberg M, Hufnagel P, Franzen J, Holle A (2003) A novel MALDI LIFT-TOF/TOF mass spectrometer for proteomics. *Anal Bioanal Chem* 376:952–965
- Süss KH, Arkona C, Manteuffel R, Adler K (1993) Calvin cycle multienzyme complexes are bound to chloroplast thylakoid membranes of higher plants in situ. *Proc Natl Acad Sci USA* 90:5514–5518
- Süss KH, Prokhorenko I, Adler K (1995) In situ association of Calvin cycle enzymes, ribulose-1, 5-bisphosphate carboxylase/oxygenase activase, ferredoxin-NADP⁺ reductase, and nitrite reductase with thylakoid and pyrenoid membranes of *Chlamydomonas reinhardtii* chloroplasts as revealed by immunoelectron microscopy. *Plant Physiol* 107:1387–1397
- Takahashi H, Ehara Y, Hirano H (1991) A protein in the oxygen-evolving complex in the chloroplasts is associated with symptom expression on tobacco leaves infected with cucumber mosaic virus strain Y. *Plant Mol Biol* 16:689–698
- Tanaka M, Wakasugi T, Sugita M, Shinozaki K, Sugiura M (1986) Genes for the eight ribosomal proteins are clustered on the chloroplast genome of tobacco (*Nicotiana tabacum*): similarity to the S10 and *spc* operons of *Escherichia coli*. *Proc Natl Acad Sci USA* 83:6030–6034
- Taylor NL, Tan Y-F, Jacoby RP, Millar AH (2009) Abiotic environmental stress induced changes in the *Arabidopsis thaliana* chloroplast, mitochondria and peroxisome proteomes. *J Proteomics* 72:367–378
- Teixeira J, Pereira S, Cánovas F, Salema R (2005) Glutamine synthetase of potato (*Solanum tuberosum* L. cv. Desiree) plants: cell- and organ-specific roles in nitrogen assimilation and mobilization. *J Exp Bot* 56:663–671
- Timperio AM, D'Amici GM, Barta C, Loreto F, Zolla L (2007) Proteomics, pigment composition, and organization of thylakoid membranes in iron-deficient spinach leaves. *J Exp Bot* 58:3695–3710
- van Wijk KJ (2001) Challenges and prospects of plant proteomics. *Plant Physiol* 126:501–508
- van Wijk KJ (2004) Plastid proteomics. *Plant Physiol Biochem* 42:963–977
- Vranová E, Inzé D, Van Breusegem F (2002) Signal transduction during oxidative stress. *J Exp Bot* 53:1227–1236
- Wales R, Nweman BJ, Pappin D, Gray JC (1989) The extrinsic 33 kDa polypeptide of the oxygen-evolving complex of photosystem II is a putative calcium-binding protein and is encoded by a multi-gene family in pea. *Plant Mol Biol* 12:439–451
- Whitelegge JP (2003) Thylakoid membrane proteomics. *Photosynth Res* 78:265–277
- Wilson KA, McManus MT, Gordon ME, Jordan TW (2002) The proteomics of senescence in leaves of white clover, *Trifolium repens* L. *Proteomics* 2:1114–1122
- Yamada S, Komori T, Hashimoto A, Kuwata S, Imaseki H, Kubo T (2000) Differential expression of plastidic aldolase genes in *Nicotiana glauca* plants under salt stress. *Plant Sci* 54:61–69
- Yamamoto Y, Tsuji H, Obokata J (1993) Structure and expression of a nuclear gene for the PSI-D subunit of photosystem I in *Nicotiana glauca*. *Plant Mol Biol* 22:985–994
- Yan JX, Wait R, Berkelman T, Harry RA, Westbrook JA, Wheeler CH, Dunn MJ (2000) A modified silver staining protocol for visualization of proteins compatible with matrix-assisted laser desorption/ionization and electrospray-mass spectrometry. *Electrophoresis* 21:3666–3672
- Zaltsman A, Feder A, Adam Z (2005a) Developmental and light effects on the accumulation of FtsH protease in *Arabidopsis* chloroplasts—implications for thylakoid formation and photosystem II maintenance. *Plant J* 42:609–617
- Zaltsman A, Ori N, Adam Z (2005b) Two types of FtsH protease subunits are required for chloroplast biogenesis and photosystem II repair in *Arabidopsis*. *Plant Cell* 17:2782–2790
- Zhou W, Eudes F, Laroche A (2006) Identification of differentially regulated proteins in response to a compatible interaction between the pathogen *Fusarium graminearum* and its host, *Triticum aestivum*. *Proteomics* 6:4599–4609